

## **Supplementary material**

to

### **Analyzing molecular current-voltage characteristics with the Simmons tunneling model: *Scaling and linearization***

by

Ayelet Vilan

#### ***S1. Translating polynomial coefficients into barrier parameter***

There are two more barrier parameters ( $\varphi_0$ ,  $m^*$ ,  $\alpha$ ,  $A$ ,  $l$ ) than mathematically distinguishable parameters ( $G_0$ ,  $\varphi_0$ , and either  $\rho$  or  $\beta_0 l$ , see equation 2). Thus, in any case one should assume at least two of the physical parameters as known. Since all the equations are related, there are few options as to which parameter is taken as known. Following is list of expressions used for translating the polynomial coefficients ( $G_0$ ,  $C$  &  $P$ ) into barrier parameters depending on the number of polynomial coefficients (1, 2 or 3). The different options are summarized in Table s1.

##### ***S1.a. Single polynomial coefficient***

Performing a simple linear fit ( $I$  vs.  $V$ ) provides a single extractable parameter ( $G_0$ ), which can be translated into the dimensionless thickness ( $\beta_0 l$ ) if all the other parameters are known. Equation 4 is rearranged and expressed in terms of  $\beta_0 l$  (instead of  $\rho\varphi_0$ ):

a) as function of contact area ( $A$ ) and barrier width ( $\alpha l$ ) – see equation a7 of main text.

b) as function of barrier height ( $\varphi_0$ ), effective mass ( $m^*$ ) and contact area ( $A$ ):

$$\beta_0 l + \ln\left(\frac{(\beta_0 l)^2}{\beta_0 l - 2}\right) = \ln(8\pi m_0 e^3 / h^3) - \ln(G_0 / A m^* \varphi_0) \quad (\text{s1})$$

c) as function of shape factor ( $\rho$ ), effective mass ( $m^*$ ) and contact area ( $A$ ):

$$\beta_0 l - \ln(1 - 2/\beta_0 l) = \ln(8\pi m_0 e^3 / h^3) - \ln(\rho G_0 / A m^*) \quad (\text{s2})$$

Note that for above equations (s1 - s2), the logarithmic term on the left side of the equality can be neglected for  $\beta_0 l \gg 2$ , providing an analytical solution to the otherwise non-analytical expressions.

### **S1.b. Two polynomial coefficients**

Equations a6 and a9 of main text's Appendix described the extraction of shape factor or barrier height (equations a8 and a9) from the two quasi-equilibrium coefficients ( $G_0$  and  $C$ ). To find  $\beta_0 l$  if  $\varphi_0$  is known, one needs to solve the cubic equation:

$$(\beta_0 l)^3 - 3(\beta_0 l)^2 - (3 + 96C\varphi_0^2)\beta_0 l + 192C\varphi_0^2 = 0 \quad (\text{s3})$$

Using equation a9 it is clear that  $\beta_0 l \approx \varphi_0 \cdot \sqrt{96C}$ . Thus, out of three possible solutions of equation s3, the most relevant one is that which is closest to this approximate value.

Alternatively, expressing  $\beta_0 l$  as a function of  $\rho$  is much simpler and allows for simpler, quadratic relations:

$$\beta_0 l = 1 + \frac{0.5 + \sqrt{5.25 - 6 \cdot \frac{96C}{\rho^2} + \left(\frac{96C}{\rho^2}\right)^2}}{\left(1 - \frac{96C}{\rho^2}\right)} \quad (\text{s4})$$

Equation s4 can be solved for both positive and negative  $C$  values. A negative  $C$  value is rather rare, but there is no mathematical restriction on the solution of s4. For positive  $C$ ,  $\rho < \sqrt{19.4C}$  to get a real solution of equation s4.

### **S1.c. Three polynomial coefficients**

Theoretically, the dimensionless thickness  $\beta_0 l$ , can be extracted from the ratio  $P/C^2$ , where  $P$  is the fifth power coefficient and  $C$  is the cubic coefficient of equation 5, by solving the following 5<sup>th</sup> order polynomial:

$$\frac{1}{3}\left(\frac{10P}{C^2} - 3\right)(\beta_0 l)^5 - 2\left(\frac{10P}{C^2} - 1\right)(\beta_0 l)^4 + \left(\frac{10P}{C^2} + 15\right)(\beta_0 l)^3 + 6\left(\frac{10P}{C^2} + 2.5\right)(\beta_0 l)^2 + 3\left(\frac{10P}{C^2} - 15\right)\beta_0 l - 90 = 0 \quad (\text{s5})$$

Generally, equation s5 has up to 5 possible solutions and a good initial guess would be  $\beta_0 l \approx (\varphi_0 = 1) \cdot \sqrt{96C}$ . After extracting a value for  $\beta_0 l$  (equation s5) this value can be used to extract  $\rho$  (equation a8), and their ratio will give  $\varphi_0$ . Now the contact area ( $A$ ) can be extracted from  $G_0$  up to a known effective mass ( $m^*$ ) or a known junction width ( $al$ ) using inversed equations 4.c (or s2) and 4.b (or a7), respectively. Nevertheless, the  $P$  coefficient was found to be not at all robust (see section 2.3.3 in text), and it is, thus, not recommended to use it.

**S1.d. Short-hand summary**

The relations between the three analytical approaches as well as the numerical one are summarized in Table s1:

**Table s1:**  
**Nutshell prescription for extracting tunneling parameters,**  
**based on the Simmons models**

	Extrac. coeff.	Translated into:					
		known $\alpha, A$	Eq	known $m^*, A$	Eq	known $\varphi_0$	Eq
Linear	$G_0$	$\beta = f(G_0, l, \alpha, A)$	a7	$\beta = f(G_0, l, m^*, A, \varphi_0)$	s1	$\beta = f(G_0, l, m^*, A, \varphi_0)$	s1
Cubic	$G_0, C$	$\beta = f(G_0, l, \alpha, A)$	a7	$\beta = f(G_0, C, l, m^*, A)$	a6	$\beta = f(C, \varphi_0, l)$	s3
		$\varphi_0 = f(G_0, C, \beta l)$	a9	$\varphi_0 = f(G_0, C, \beta l)$	a9	$m^* A = f(G_0, \varphi_0, \rho)$	4.c
5 <sup>th</sup> order	$G_0, C, P$	$\beta = f(C, P, l)$	s5	$\beta = f(C, P, l)$	s5	$\beta = f(C, P, l)$	s5
		$\varphi_0 = f(G_0, C, \beta l)$	a9	$\varphi_0 = f(G_0, C, \beta l)$	a9	$m^* = f(\beta l, \varphi_0)$	a1
		$A/\alpha^2 = f(G_0, \rho)$	4.b	$m^* A = f(G_0, \varphi_0, \rho)$	4.c	$A = f(G_0, \varphi_0, \rho, m^*)$	4.c

## S2. Additional numerical fitting maps

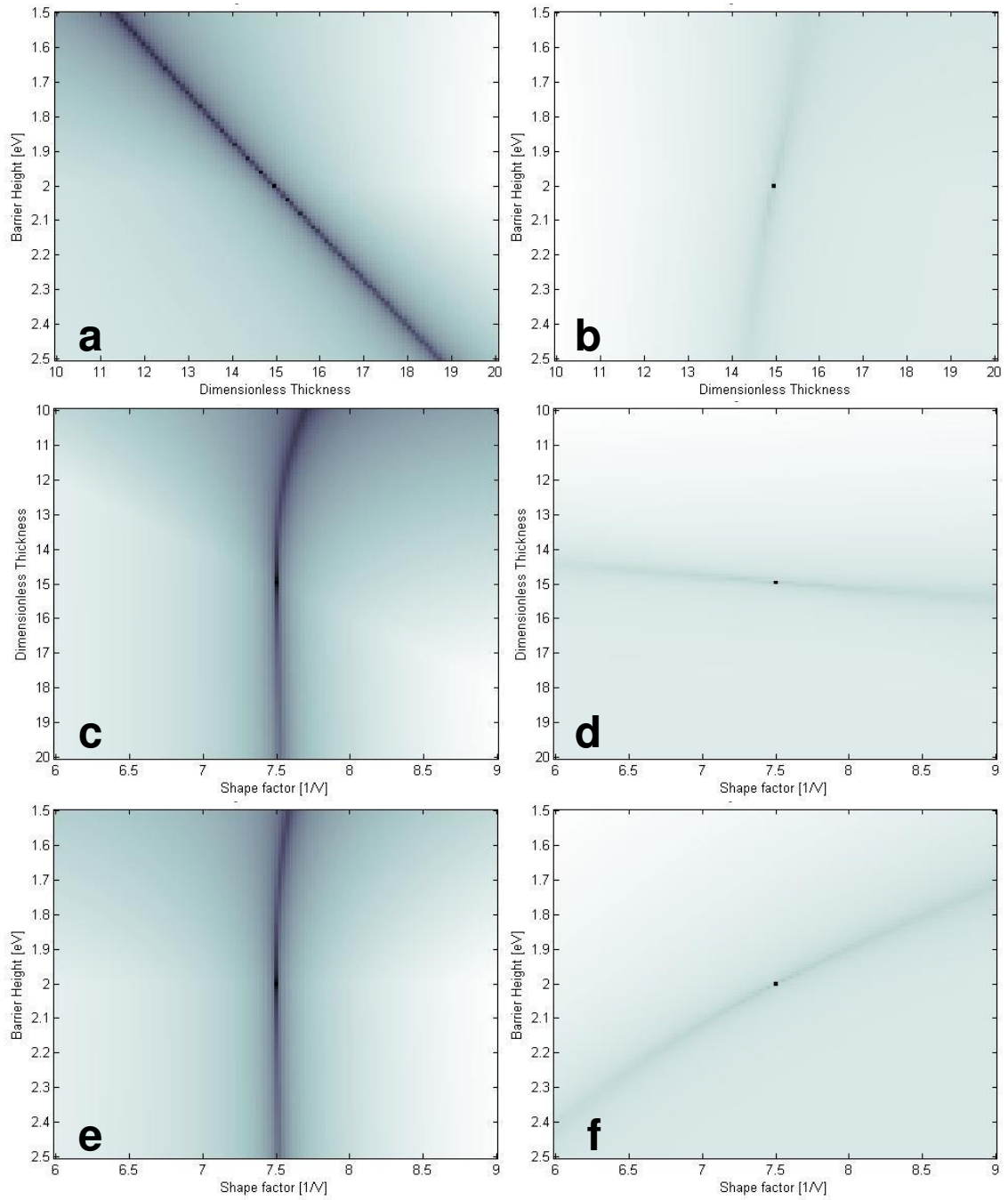


**Figure s1:** MSE maps with additional parameter couples as coordinates (*cf.* Figure 2, main text). The left column is for constant  $G_0$  (Figure 2.b) and the right column is for constant  $A$  (Figure 2.c). The coordinate sets are:  $\varphi_0 - \beta l$  (**a,b**);  $\beta l - \rho$  (**c,d**); and  $\varphi_0 - \rho$  (**e,f**). See legend to Figure 2 for more details.

The set of fitting parameters of panels (**a**) and (**f**) is correlated, as evident by the diagonal valley direction. Panels (**e**) and (**b**) are identical to panels (**b**) and (**c**), respectively of Figure 2.

### S3. Comparison of extracted parameters between different procedures

**Table s2:**

Summary of junction parameters extracted by different procedures for octane dithiol single molecule contacted by gold nano particle and CP-AFM

		Range [V] <sup>a)</sup>	$G_0$ [nS] <sup>b)</sup>	$\rho$ [V <sup>-1</sup> ] <sup>c)</sup>	$\beta_0$ <sup>d)</sup>	$\varphi_0$ [V] <sup>e)</sup>	$m$ <sup>* f)</sup>	$A$ [Å <sup>2</sup> ] <sup>g)</sup>
0	Reference values <sup>h)</sup>		0.003	4.8	0.79	1.42	0.16	22.0
	Fit order	Linearized fit						
1	1 <sup>st</sup> order	0.01	0.94	4.8	0.40	0.96	0.16	22
2	3 <sup>rd</sup> order	0.10	1.04	25.0 (21.1)	0.40 (0.36)	0.28 (0.30)	0.54 (0.41)	22
	Input parameter	Known $G_0$						
3	$G_0$ <sup>j)</sup>	1.00	0.94	11.9	0.27	0.41	0.18	4.2
4	$G_0, C$ <sup>k)</sup>	1.00	0.93	22.9	0.59	0.17	2.03	384
	Input parameter	Known $A$						
5	$A/l^2$ <sup>i)</sup>	1.00	1.43	8.8	0.37	0.74	0.18	22
6	$A/l^2, G_0$ <sup>ij)</sup>	1.00	0.94	10.1	0.40	0.70	0.22	22
7	Variance <sup>l)</sup>		21%	102% (20%)	33% (7%)	71%	112%	68%

- The span of the fitting range was arbitrary for entries 1-2, and was the full measurement range for entries 3-6. In case of apparently non-physical results, the 'full range' was limited to 0.25 V.
- Calculated using equation 4.b for entries 0 & 5 and extracted graphically otherwise;
- Calculated based on the cubic parameter,  $C$  and equation a8 for entry 4 (values in brackets are based on the approximated equality of equation a8), and, otherwise  $\rho \equiv \beta_0 l / \varphi$  or using equation 3.
- Calculated for molecular length of  $l = 17.6 \text{ \AA}$  and  $\alpha \equiv 1$ , using equations a1 (entry '0'), or from  $G_0$  and equation a7 (1<sup>st</sup>, 2<sup>nd</sup> entries). For entries 3-6 the product  $\beta_0 l$  was a fitting parameter. Values in brackets are approximated ones, based on equation a6.
- Calculated from equation a9 and previous values (previous values in brackets);
- Calculated from equation a1 and previous values assuming  $\alpha \equiv 1$ ;
- Calculated from equation 4.b and previous values assuming  $\alpha \equiv 1$ ;
- Reference values are taken from original publication, ref. 18;
- $A/l^2$  taken from entry '0';
- $G_0$  taken from entry '1';
- $G_0$  &  $C$  taken from entry '2';
- Calculated as standard deviation divided by average, with logarithmic averaging for contact area; value in brackets – for  $\rho$ : limited to quasi-equilibrium (entries '2' & '4'); for  $\beta_0$ : to known contact area (entries '1', '2', '5' & '6');

**Table s3:**

Summary of junction parameters extracted by different procedures for dodecane thiol monolayer in a gold nano-pore. Change order of tables and relevant main text.

		Range [V] <sup>a)</sup>	$G_0$ [nS] <sup>b)</sup>	$\rho$ [V <sup>-1</sup> ] <sup>c)</sup>	$\beta_0$ <sup>d)</sup>	$\phi_0$ [V] <sup>e)</sup>	$m^*$ <sup>f)</sup>	A [nm <sup>2</sup> ] <sup>g)</sup>
0	Reference values <sup>h)</sup>		10.4	10.1	0.79	1.42	0.42	1600
	Fit order	Linearized fit						
1	1 <sup>st</sup> order	0.05	4.7	10.1	0.84	1.60	0.42	1600
2	3 <sup>rd</sup> order	0.10	4.2	34.4 (32.8)	0.84 (0.78)	0.45 (0.43)	1.52 (1.35)	1600
	Input parameter	Known $G_0$						
3	$G_0$ <sup>j)</sup>	0.25	4.2	35.2	0.46	0.24	0.86	3.3
4	$G_0, C$ <sup>k)</sup>	0.25	4.2	34.7	0.76	0.40	1.38	386
	Input parameter	Known A						
5	$A/l^2$ <sup>i)</sup>	1.00	5.8	14.5	0.82	1.04	0.62	1600
6	$A/l^2, G_0$ <sup>i,j)</sup>	1.00	4.2	15.4	0.84	1.00	0.68	1600
7	Variance <sup>l)</sup>		17%	98% (7%)	40% (4%)	81%	51%	128%

Notes identical to Table s1, except for:

d) Calculated for molecular length of  $l = 18.2 \text{ \AA}$ ;

h) Reference values are taken from original publication, ref. 14;

**Table s4:**

Summary of junction parameters extracted by different procedures for a bilayer of docosanethiol, contacted by a floating gold flake.

		Range [V] <sup>a)</sup>	$G_0$ [nS] <sup>b)</sup>	$\rho$ [V <sup>-1</sup> ] <sup>c)</sup>	$\beta_0$ <sup>d)</sup>	$\phi_0$ [V] <sup>e)</sup>	$m^*$ <sup>f)</sup>	A [ $\mu\text{m}^2$ ] <sup>g)</sup>
0	Reference values <sup>h)</sup>		0.0001	15.4	0.79	1.42	0.16	50
	Fit order	Linearized fit						
1	1 <sup>st</sup> order	0.01	123.0	15.4	0.39	0.89	0.16	50
2	3 <sup>rd</sup> order	0.10	129.6	49.3 (47.8)	0.39 (0.37)	0.42 (0.42)	0.34 (0.32)	50
	Input parameter	Known $G_0$						
3	$G_0$ <sup>j)</sup>	0.50	123.0	20.7	1.40E+06	3.55E+06	2.09E+06	Inf
4	$G_0, C$ <sup>k)</sup>	0.50	32.0	100.3	0.08	0.04	0.14	8.9 nm <sup>2</sup>
	Input parameter	Known A						
5	$A/l^2$ <sup>i)</sup>	0.50	38.1	16.9	0.41	1.28	0.50	50
6	$A/l^2, G_0$ <sup>i,j)</sup>	0.50	30.8	21.0	0.41	1.05	0.62	50
7	Variance <sup>l)</sup>		44%	83% (18%)	64% (5%)	86%	50%	722%

Notes identical to Table s2, except for:

d) Calculated for molecular length of  $l = 53.1 \text{ \AA}$ ;

h) Reference data are based on nominal contact area, molecular length, and other published data (barrier height<sup>14</sup> and effective mass<sup>18</sup>);

#### ***S4. Detailed description on preparation of bilayer alkyl thiols junction***

Figure s2 shows an image of the reported junction, prepared by floating the flakes on the molecules (s2.a), its schematic cross-section (s2.b) and suggested equivalent electrical circuit (s2.c).

**Gold flakes** of 50 nm thick and 5 by 50  $\mu\text{m}$  wide were lithographically patterned over a release layer<sup>1</sup>. Before use, the release layer is dissolved and the flakes are suspended in an organic solvent such as dichloromethane. Dissolved residuals of the release layer are removed by 3 cycles of centrifuging, decanting and suspending of the flakes. Finally the suspending liquid is replaced by a 2 mM ethanol solution of 1-docosanethiol ( $\text{HS}(\text{CH}_2)_{21}\text{CH}_3$ ). The resulting flake suspension in ethanol was stable for at least one month, but normally used within a few days, but at least one hour after preparation to allow complete thiol adsorption.

**Fixed electrodes (substrate)** were patterned as sets of two interdigitated electrodes by standard lithography and evaporation of 50 nm thick Au over 10 nm Ti (adhesion layer) over 230 nm of a thermally grown oxide on top of a highly doped n-Si wafer. The substrates were stored in air up to several months and cleaned immediately before use by 1 min immersion in fuming nitric acid, plunged into DI water, dried by a  $\text{N}_2$  jet and subjected to UV-ozone for 10 min. The substrate is then immediately immersed in 2 mM ethanol solution of 1-docosanethiol for 1-3 hours. After adsorption, an excess molecule is removed by immersion in clean ethanol for 30 sec, rinsing with jets of ethanol and heptane and dried by a  $\text{N}_2$  jet. Flakes were then deposited immediately.

**Placing the flakes on the substrate.** The flakes are cleaned from excess thiols by centrifuging, decanting, and suspending them in ethanol for three times to ensure the removal of any residual, non-bonded molecules. The flakes are then suspended in neat ethanol for minimal duration to reduce molecule desorption from the flakes. From one up to a few drops of the final suspension are placed on the monolayer-covered substrate and allowed to dry naturally. The concentration of flakes in the final suspension dictates the resulting density of flakes per substrate area.

**Electrical characterization:** The substrate with flakes was placed in a probe station and its microscope was used to detect a set of interdigitated electrodes (see Figure s2.d), which is crossed by a single flake. It was then contacted by micromanipulators and the current-voltage characteristics were measured with an Agilent 4155 parameter analyzer.

The resulting device is a “double” one, meaning that it includes two junctions in series, as schematically drawn in Figure s2.c. The basic molecular junction (metal/monolayer1/monolayer2/ flake) is described by a diode, to indicate possible asymmetry in it. If such asymmetry really exists it must be opposite for the two sides of the flakes, thus the net device is expected to behave symmetrically, and we can not deduce from the seemingly symmetric *I-V* characteristics whether the single junction is symmetric or rectifying, where in the first case the applied bias is divided equally over the two junctions in series and in the second case most of the bias falls on the diode in the reverse direction at each biasing. Chemically the junction is completely

---

<sup>1</sup> Hikmet, R. A. M., patent No. WO 2005085389; Koninklijke Philips Electronics N.V., Neth. **2005**

symmetric. Therefore, we followed the symmetric assumption and consider the actual bias at each junction to be half of the nominal applied bias.

These types of junctions were produced and measured by AV in the research division of **Philips Electronics**, Netherlands.

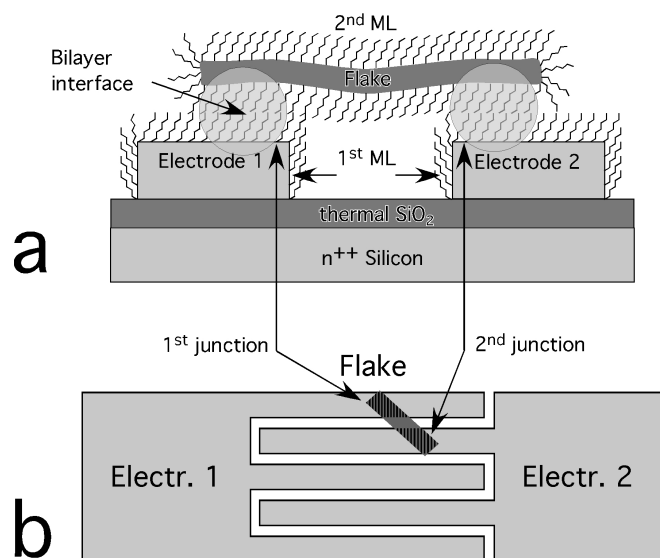


**Figure s2:** Schematic drawing and image of the flakes molecular junctions.

- a) A schematic side view of the junction, showing two permanent Au electrodes (Electrode 1 and 2) on top of a SiO<sub>2</sub> insulator and n<sup>++</sup>-Si substrate. A metal flake bridges between the two electrodes, and both the flake and the permanent electrodes are covered with a monolayer of molecules (the flake is covered on both sides with the monolayer). The transparent circles represent the bilayer interface and junction area;
- b) Top view of the same junction showing the interdigitated nature of the permanent electrodes, with arrows indicating the junction areas.
- c) Suggested equivalent electrical circuit (see text) and the measurement configuration.
- d) An optical image of a typical bilayer junction (similar to scheme

c) showing one flake crossing two electrodes (bright color). The junction areas again are marked by circles. The large bright area on the left side is the contacting pad, and dark stripes are the insulating SiO<sub>2</sub>. Additional flakes, that do not bridge electrodes, can be

seen on the contacting pad at the top, middle and bottom.